MULTISCALE STRUCTURAL STUDY OF METAOPHIOLITE OF VAL D'ALA, NORTHERN SLOPE (PIEMONTE ZONE - WESTERN ALPS - ITALY)

Matteo Assanelli* and **Manuel Roda*,**[✉]

* *Università degli Studi di Milano, Dipartimento di Scienze della Terra "A. Desio", Milano, Italy.*
[✉]*Corresponding author, e-mail: manuel.roda@unimi.it*

ABSTRACT

This contribution presents a geological and structural study of the Val d'Ala metaophiolite complex (Lower Piemonte Zone) at the southern boundary of the Gran Paradiso Massif. Although this area was known since the 18th century for mining activity, a complete and modern multiscale structural study of the metaophiolite is still lacking. For this reason, we realized a structural map at 1:10,000 scale along the northern slope of middle Val d'Ala and we completed the study with a microstructural analysis. Here, serpentinites and metabasites are the dominant rocks and host hectometre-sized calcschist bodies, metre to decametre-sized metagabbro bodies, and some metre-sized eclogite lenses. All these lithologies belong to the Lower Piemonte Zone. In the upper part of the northern slope of the valley the tectonic contact with the gneisses of the Gran Paradiso Massif occurs. Four groups of superposed structures have been recognized by the multiscale investigation of the cross-cutting relationships between minerals, foliations, and folds. D_1 relict fabrics occur in eclogites, metagabbros, and metabasites and are marked by omphacite, garnet, rutile, and glaucophane. Oldest metamorphic relics in serpentinites are serpentine and rare amphibole, in calcschists are quartz and calcite, and in gneisses are quartz, garnet, and plagioclase. D_2 structures consist of isoclinal folds and the S_2 axial plane foliation that represents the dominant fabric and developed within all rock types. The S_2 foliation is marked by glaucophane and epidote in the metabasites, metagabbros, and eclogites, serpentine and chlorite in the serpentinites, carbonate, quartz, white mica in the calcschists and quartz, plagioclase, and white mica in the gneisses. Locally green amphibole, chlorite and plagioclase replace omphacite and glaucophane. The lithological boundaries and the tectonic contact between the Piemonte Zone metaophiolite and the gneisses of the Gran Paradiso Massif is parallel to S_2. The D_3 structures consists of a fold system with sub-horizontal axial plane (PA_3) and axis (A_3). The D_4 fabric consists of isoclinal to open folds with sub-vertical dipping axial plane (PA_4) and sub-horizontal axis (A_4). D_1 mineral assemblage suggests a metamorphic peak under eclogite-facies conditions for the metaophiolite complex, followed by re-equilibration under blueschist-facies conditions in which the contact with the gneisses of the Gran Paradiso Massif developed. The two units evolved together in lower pressure and temperature conditions.

INTRODUCTION

Structural mapping and analysis of metamorphic basements are fundamental tools for deciphering the relationships between the development of deformation fabrics and metamorphic reactions that in turn allow the reconstruction of the tectono-metamorphic evolution of polydeformed rocks. Modern structural techniques of metamorphic basements include the description of meso and microscopic fabrics considering their mineralogical supports, which testify the metamorphic conditions under which the deformation developed (Myers, 1978; Passchier et al., 1990; Spalla et al., 2000: 2005; Zucali et al., 2002; Spalla and Zucali, 2004; Salvi et al., 2010; Roda and Zucali, 2011; Gosso et al., 2015; Cantù et al., 2016).

We present here a multiscale structural study of the metaophiolite complex of middle Val d'Ala (Piemonte, Italy), one of the Lanzo valleys, in the axial part of the subduction complex of the Western Alps (Fig. 1; SM1). Although since the 18th century Val d'Ala is internationally renowned for mining activity of minerals as garnet, diopside, vesuvianite, and epidote (Diella et al., 2019), and the tectonic contact between Piemonte Zone and Gran Paradiso Massif is well exposed (Bigi et al., 1990), a detailed modern structural analysis of the area is still lacking. First geological and petrological works on the metaophiolite complex focused on the lithological description and petrochemical investigation of mafic and ultramafic rocks (Nicolas, 1966; Leardi et al., 1984; Leardi and Rossetti, 1985). The accurate geological map of Leardi and Rossetti (1985) represented a fundamental geological support for the sampling and from this study

the first estimation of metamorphic peak conditions under eclogite-facies conditions resulted (P=1.3 GPa, T=450-460°C, Sandrone et al., 1986). However, structural data and fabric elements (at meso and microscale) were not presented in these works. Only recently, a structural-geological map of the middle Val d'Ala presented new structural data of the metaophiolite complex at the contact with the Gran Paradiso Massif (Caso et al., 2021).

GEOLOGICAL SETTINGS

The investigated area is in the Western Alps, on the northern side of Val d'Ala, at the contact between the Lower Piemonte Zone and the Gran Paradiso Massif (Fig. 1). The Alps developed because of the collision between European and Adria plates after the subduction of the Alpine Tethys Ocean, during Cretaceous-Oligocene times (Reddy et al., 1999; Dal Piaz, 2010; Lardeaux, 2014; van Hinsbergen et al., 2020; Agard and Handy, 2021). The axial zone of the Western Alps (Fig. 1a), i.e., the section of the Alpine chain between the Periadriatic Fault System and the Penninic Front, contains units of continental and oceanic origin that belong to both Austroalpine and Pennine domains and are tectonically mixed during burial and exhumation consequent to the Alpine convergence (Dal Piaz et al., 1972; Caron et al., 1984; Polino et al., 1990; Reddy et al., 1999; Schmid et al., 2004; Roda et al., 2012; Lardeaux, 2014). The Austroalpine domain consists of continental rocks tectonically scraped off by the margin of Adria plate, subducted, and exhumed during the
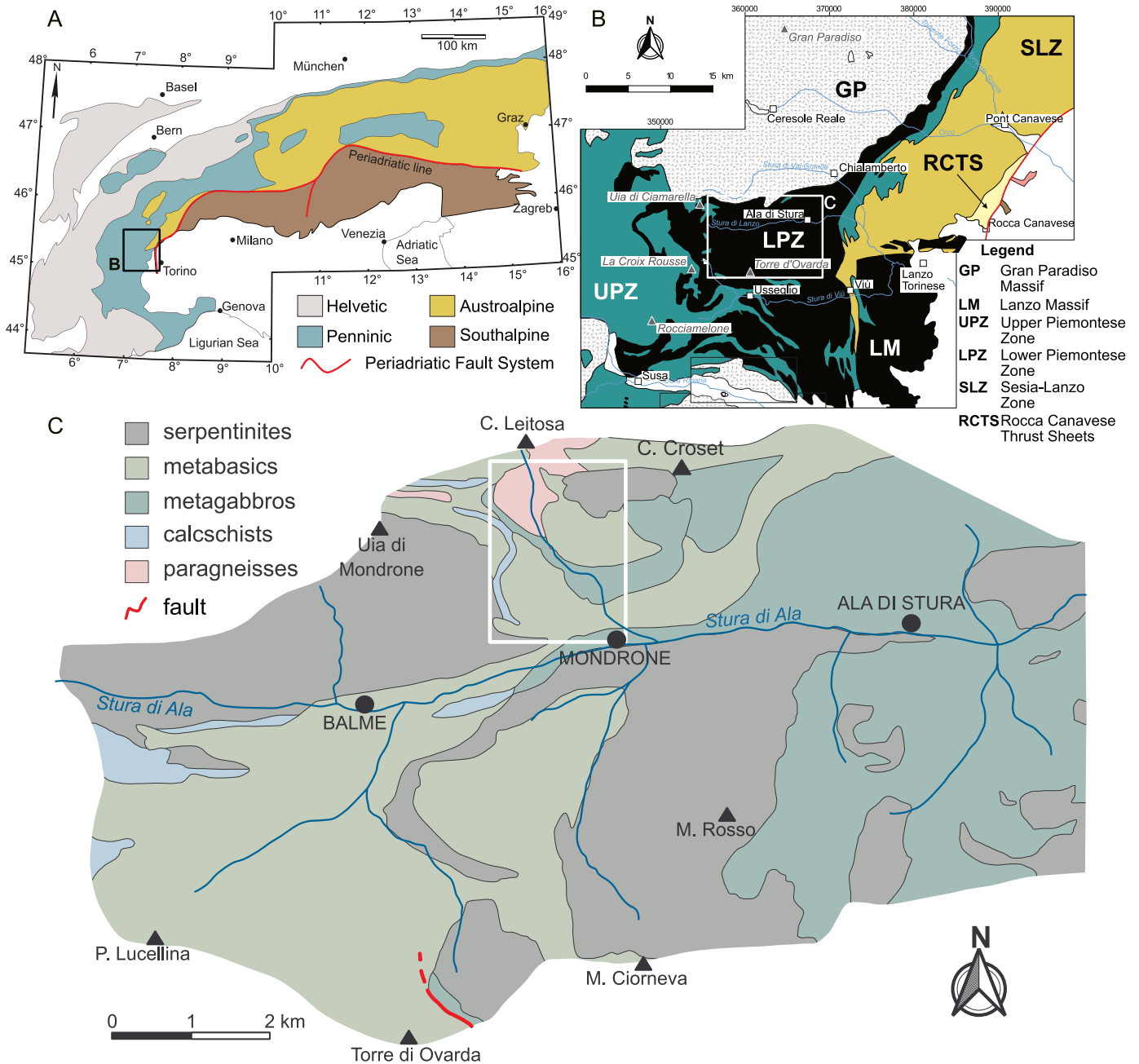
Fig. 1 - Geological setting: a) Simplified tectonic scheme of the Alps with the different structural domains. Redrawn after Bigi et al. (1990). Coordinate system WGS84 UTM Zone 32. The black rectangle locates the tectonic map in (b). b) Simplified tectonic map of the southern Western Alps. The white rectangle locates the lithological map in (c). c) Simplified lithological map of Val d'Ala redrawn after Sandrone et al. (1986) and Diella et al. (2019). The study area is located by the white rectangle.

Alpine subduction (Spalla et al., 1996; Babist et al., 2006; Roda et al., 2012; 2020).

The Pennine domain consists of continental rocks that belong to the European margin (Briançonnais Units and Internal Crystalline Massifs) and oceanic and metasedimentary rocks that represent remnants of subducted Alpine Tethys oceanic lithosphere (Piemonte Zone).

The Briançonnais Units (Fig. 1a) form a continuous exposure of continental basement and Mesozoic/Tertiary cover rocks bordering the Piemonte Zone to the east and the Helvetic Domains to the West (Escher et al., 1997; Michard et al., 2004; Malusà et al., 2005). A general increase in metamorphic grade from low-greenschist- to epidote blueschist-facies conditions is observed from the western to the eastern units (Bousquet et al., 2008).

The Internal Crystalline Massifs comprise the Monte Rosa, Gran Paradiso, and Dora-Maira Massifs. These massifs consist of a Variscan basement with a Carboniferous metamorphic imprint under amphibolite-facies conditions, intruded by Permian granitoids (Dal Piaz, 1966; Callegari et al., 1969; Compagnoni and Prato, 1969; Compagnoni et al., 1974; Sandrone et al., 1988; 1993; Bertrand et al., 2005). The Internal Crystalline Massifs recorded an Alpine metamorphic peak under eclogite- and blueschist-facies conditions of Eocene age, followed by greenschist to amphibolite-facies re-equilibration (Pognante and Sandrone, 1989; Chopin et al.,

1991; Borghi et al., 1996; Rolland et al., 2000; Le Bayon et al., 2000; Le Bayon R.et al., 2006; Castelli et al., 2007; Lapen et al., 2007; Gasco et al., 2010; 2011b; 2011a; 2013; Gabudianu Radulescu et al., 2011; Manzotti et al., 2015). In particular, the Gran Paradiso Massif (GP) is composed by two main tectonic units. The upper one (Gran Paradiso Unit) is made of poly-metamorphic metasediments (Alpine and Variscan cycle) intruded by Permian granitoids and both transformed during the Alpine history into para and orthogneisses respectively. These lithologies record eclogite-facies conditions, partially overprinted by albite-amphibolite facies minerals (Le Bayon B. et al., 2006; Gasco et al., 2010; Manzotti et al., 2015; 2018). The lower unit (Money Unit) consists of mono-metamorphic (Alpine) metasediments and metavolcanics rocks intruded by the Permian Erfaulet granite. Alpine peak P–T conditions were attained at lower pressure compared to the Gran Paradiso Unit (Gasco et al., 2010; Manzotti et al., 2015; 2018). The two units coupled together under blueschist-facies conditions and exhumed sharing three deformation stages characterized by three folding phases and two axial plane foliations (Manzotti et al., 2015).

The Piemonte Zone is divided in Upper (External) and Lower (Internal) Piemonte zones (Fig 1b), that in the northern part of the Western Alps correspond to Combin and Zermatt-Saas zones, respectively (Martin et al., 1994; Gasco et al., 2013). The Upper Piemonte Zone consists of carbonate to terrigenous flysch-type metasediments, commonly including metaophiolite bodies (Dal Piaz et al., 1981; Dal Piaz, 1988; Gasco et al., 2013). The latter are locally covered by manganiferous quartzites and other oceanic sediments (Dal Piaz et al., 1979; Vannay and Allemann, 1990). The dominant metamorphic imprint is recorded under greenschist- to blueschist-facies conditions attained at 36-40 Ma (Kienast, 1983; Dal Piaz, 1988; Vannay and Allemann, 1990; Martin and Cortiana, 2001; Gouzu et al., 2016), although recent analyses on serpentinites suggest eclogite-facies conditions for the metamorphic peak just to the north of Val d'Ala, at the contact between Piemonte Zone and Sesia-Lanzo Zone (Assanelli et al., 2020). The Lower Piemonte Zone consists of ultramafic and mafic metaophiolite sequences and minor associated metasedimentary covers. Serpentinites are the most abundant rocks, often enclosing rodingite dikes and metagabbro bodies (Bearth, 1967; Dal Piaz and Ernst, 1978; Rahn and Bucher, 1998; Li et al., 2004a; Groppo and Compagnoni, 2007; Fontana et al., 2008; 2015; Rebay et al., 2012; Zanoni et al., 2012; 2016). Mafic rocks are Mg- and Fe- gabbros and metabasalts with a normal-MORB signature and recorded a HP-UHP dominant metamorphic imprint (Martin et al., 1994; Bucher et al., 2005; Bucher and Grapes, 2009; Balestro et al., 2019; Bucher and Stober, 2021). The metasedimentary covers consist of quartzites, marbles and calcschists that recorded an eclogite-facies metamorphic imprint (Dal Piaz et al., 1979; Bearth and Schwander, 1981; Barnicoat and Fry, 1986; Reinecke, 1991; Angiboust et al., 2009; Groppo et al., 2009; Weber and Bucher, 2015; Tartarotti et al., 2019), and locally UHP assemblages have been recognized (Reinecke, 1991; Frezzotti et al., 2011; Luoni et al., 2018; 2019). The protolith ages inferred from oceanic gabbros and peridotites cluster around approximately 160 Ma (Mevel et al., 1978; Li et al., 2013; Tribuzio et al., 2016; Roda et al., 2018b; Nicollet et al., 2022) and the HP metamorphism is generally dated between 70 and 40 Ma (Reddy et al., 1999; Rubatto et al., 1999; Lapen et al., 2003; Skora et al., 2009; de Meyer et al., 2014; Gouzu et al., 2016; Rebay et al., 2018; Dragovic et al., 2020). The metaophiolite of Val d'Ala is part of the Lanzo Valley ophiolite (LVU) which occurs between Dora Maria and Gran Para-

diso massif. The ophiolite consists of serpentinites enclosing metagabbro and eclogite bodies, fine-grained metabasites, and metasediments as quartzites, marbles and calcschists (Nicolas, 1966; Leardi and Rossetti, 1985; Caso et al., 2021; De Togni et al., 2023). Generally, four Alpine deformation stages have been described corresponding to a metamorphic evolution from eclogite-facies up to greenschist-facies conditions (Sandrone et al., 1986; Rolland et al., 2000; Caso et al., 2021; De Togni et al., 2023).

ANALYTICAL TECHNIQUES AND SOFTWARE

The structural analysis of polydeformed metamorphic terrains uses the intersection relationships between the different superposed structures, both ductile and brittle, that are generated during different deformation stages to determine the relative chronology of the geologic and tectonic history. Here, the relative chronology of the structures was inferred from structural correlation criteria, widely used in various terrains (Turner and Weiss, 1963; Ramsay and Huber, 1983; Williams, 1985; Twiss and Moore, 1992; Passchier and Trouw, 2005; Pollard and Fletcher, 2005; Roda et al., 2018a; Zucali et al., 2020). All rocks are described and mapped considering their mineral composition, the type of planar and linear structural elements (e.g., foliation, lineation, etc.) and their corresponding mineral support. Each group of structures is attributed to a relative chronologic family (D_1, D_2, etc.) and characterized by fabric elements (e.g., S_1, S_2, etc.) with the supporting mineral association. Lithologic subdivisions are based and revised starting from the work of Leardi and Rossetti (1985). The rocks show three different fabrics, allowing the identification of finite strain states and fabric gradients: (i) Coronitic, weak syn-metamorphic foliation, preserving 80-100% of the textural primary features (mainly igneous); (ii) Tectonitic, syn-metamorphic foliation preserving 20-80% of the textural primary features; (iii) Mylonitic, syn-metamorphic foliation preserving 0-20% of the textural primary features (Spalla et al., 1998; 2005; Zucali et al., 2002; 2020; Spalla and Zucali, 2004; Salvi et al., 2010).

The geological and structural data were collected at 1:5000 scale, compiled in a GIS database (QGis - https://www.qgis.org) and represented on a topographic map extrapolated from the Carta Tecnica Regionale Vettoriale of the Regione Piemonte (BDTRE "Base Dati Territoriale di Riferimento degli Enti piemontesi", Edition 2019). The shape of the outcrops has been improved using the orthophotos of the area and the lithologic map of Leardi and Rossetti (1985), and refined with Affinity Designer 2.

The geological map (Fig. 1S) covers an area of almost 5 km², and the geological and structural data have been here represented at 1:10000 scale (SM1). The local structural architecture and the geometry of the contact between the Piemonte Zone rocks and the Gran Paradiso Massif are given in cross sections. The orientation of structural elements has been analyzed and represented by equal area lower-hemisphere stereographic projections using Stereonet (Allmendinger et al., 2013; Cardozo and Allmendinger, 2013).

We here present two different maps. In the solid and drift map, the objective outcrops delimitation and the structural elements are represented while in the interpretative map, the interpretation of lithological and structural setting of the area is synthetized based on lithological contacts, fabric element attitudes, and structural correlation criteria. We supported the geological interpretation with geometric interpolations by

using the QGis plugins qprof (https://gitlab.com/mauroalberti/qProf) and qgsurf (https://github.com/mauroalberti/qgSurf).

LITHOSTRATIGRAPHY

Along Val d'Ala, serpentinites and metabasites are the dominant rock types and include hectometre-sized calcschist bodies, metre to decametre-sized metagabbro bodies, and some metre-sized eclogite lenses (Fig. 1c; Leardi and Rossetti, 1985). These rocks belong to the Lower Piemonte Zone (Fig. 1b). In the upper part of the north slope of the valley the tectonic contact with the gneisses of the Gran Paradiso Massif occurs (Fig. 1b).

Metabasites are medium to fine-grained pale to dark green foliated rocks. The foliation is marked by alternating millimetre-thick omphacite- (5-40%), amphibole- (20-30%), garnet- (5-10%) rich and epidote- (5-10%), plagioclase- (5%), minor white mica-, chlorite-, rutile-rich layers. Dark green metabasites are rich in glaucophane and rutile (Fig. 2b). Locally, coarse-grained metabasites have a coronitic texture. At the contact between serpentinites and metabasites, a reaction rim formed by talc, serpentine, and amphibole commonly occurs.

Metagabbros are light- to dark-grey rocks with a tectonitic to coronitic texture and medium- to large grain size (Fig. 2c). They are mineralogically similar to the metabasites but, in the coronitic types, the original igneous texture is still preserved and some magmatic-relict minerals as clinopyroxene and plagioclase can be locally observed. In the tectonitic types, a discontinuous foliation is marked by alternating millimetre-thick omphacite- (30-40%), amphibole- (20-30%), garnet- (5-10%) rich and millimetre-thick plagioclase- (5%), epidote- (5-10%), minor rutile- (5%) rich layers.

Eclogites consist of coarse to medium-grained green massive metre to decametre-sized lenses within metabasites and metagabbros. They show a coronitic to tectonitic texture with a discontinuous foliation marked by alternating millimetre- to centimetre thick omphacite- (30-40%), garnet- (20-30%)-rich and glaucophane- (25%), epidote- (20%), rutile- (10%) rich layers. Locally green amphibole, chlorite and plagioclase replace omphacite and glaucophane (Fig. 2d).

Serpentinites are dark green, or pale green when altered, very fine- to fine-grained rocks with a pervasive foliation, locally mylonitic (Fig. 2a). The foliation is marked by serpentine (70-90%), amphibole (10-15%), spinel, chlorite, and talc (5%).

Calcschists are light-brown fine-grained foliated rocks consisting of calcite (70-80%), quartz (10-20%), white mica (10%), minor garnet, epidote, chlorite, and some opaque and iron minerals. The foliation, locally mylonitic, is marked by layering of millimetre to decimetre-thick carbonate-rich lithons and millimetre-thick quartz-white mica-rich films (Fig. 2e).

Gneisses are light-grey medium to fine-grained foliated rocks characterized by a spaced foliation marked by alternating millimetre to centimetre-thick quartz- (5-25%), feldspar- (20-30%), garnet- (10-15%) rich and white mica- (10-30%), minor biotite-, chlorite- (5%) rich layers (Fig. 2f).

MESOSTRUCTURAL ANALYSIS

A sequence of four deformation stages has been inferred by the investigation of the cross-cutting relationships between minerals, foliations, and folds. Serpentinites and calcschists well record deformation stages and preserve different superposed structures. On the other hand, coronitic and tectonitic rocks as eclogites and metagabbros well preserve older fabrics.

The lithological contacts are well observable between metabasites and metagabbros, and between calcschists and metabasites and they are parallel to the S_2 foliation (Fig. 3b ,c). The first group of structures (D_1) is partially to largely overprinted by the successive deformation imprints. D_1-relics occur in metabasites as decimetre-sized lenses in which the S_1 foliation is preserved (Fig. 3a) and calcschists as folded S_1 foliation. The D_1 mineral assemblage is preserved in eclogites, coronitic to tectonitic metagabbros, and metabasites and is characterized by omphacite, garnet, rutile, and amphibole (glaucophane) porphyroclasts.

During the second deformation stage (D_2) the regional fold axial plane foliation S_2 developed in both Piemonte Zone and Gran Paradiso Massif rocks. S_2 is generally spaced and locally mylonitic (mainly in serpentinites and calcschist, Fig. 3b), smooth to wriggly and with millimetre (in serpentinites and calcschists) to centimetre-sized (in metabasites and eclogites) spacing. Serpentine marked the S_2 mylonitic foliation in the serpentinites, generally with an S-C' geometry indicating top-to-NW sense of shear at present (Fig. 3d). In the metabasites, S_2 is defined by SPO of omphacite, glaucophane, garnets, and epidotes. Locally, some shear bands with mylonitic texture develop in which veins filled by epidote are transposed and boudinaged and the lenses containing the S_1 foliation are wrapped by S_2 forming sigmoids. At present, these elements indicate a top-to-NW sense of shear (Fig 3a). In the eclogites and metagabbros the S_2 tectonitic foliation is defined by SPO of omphacite and amphibole, and millimetre to centimetre-thick omphacite-, amphibole-, garnet-rich layers that alternate with millimetre-thick plagioclase-, epidote-, minor rutile-rich layers. Locally green amphibole, chlorite and plagioclase replace omphacite and glaucophane. In the calcschists, the S_2 foliation is spaced and marked by centimetre-thick carbonate-, quartz-, and minor epidote-, and garnet-rich lithons and with millimetre-thick mica and minor chlorite-rich films (Fig. 3b). Rare relicts of D_2 folds occur in carbonate-rich layers where the S_2 foliation is less pervasive (Fig. 4b). In the gneisses, S_2 is spaced and marked by millimetre to centimetre-thick quartz, plagioclase, and garnet-rich lithons and millimetre-thick white mica films. The S_2 foliation has a mainly dip direction toward SSW with dip increasing from the north to the south. The tectonic contact between the Piemonte Zone metaophiolitic rocks and the gneisses of the Gran Paradiso Massif are parallel to the S_2 attitude, and it is characterized by overthrusting of metaophiolite on gneisses. At the contact, quartz-fiber slickensides indicating a W-E movement direction can often be observed (Fig. 3e) together with small and highly deformed serpentinite lenses (Fig. 4a).

The third deformation stage (D_3) developed a fold system with open to isoclinal interlimb angle and a variable wavelength that spread from centimetre- to decametre-sized, as a function of the lithology (Fig. 4b, c, d). The axial plane (PA_3) and axis (A_3) are both sub-horizontal with variable dip direction (Fig. 5c). During this stage some parasitic folds develop and are clearly visible along the limbs and near the fold hinges. The superposition between previous fold and D_3 folding generated a type 3 interference pattern (Fig. 4b; Ramsay, 1967).

The fourth deformation stage developed open folds with a large range of wavelength from centimetre- to hectometre-sized, as a function of the lithology (Fig. 4a, d, e, f). The axial plane (PA_4) is generally sub-vertical dipping toward NE and SW directions in the southern part of the map and WNW-ENE in the northern part. The fold axis (A_4) is sub-horizontal with NW and SE dip directions (Fig. 5d). The superposition
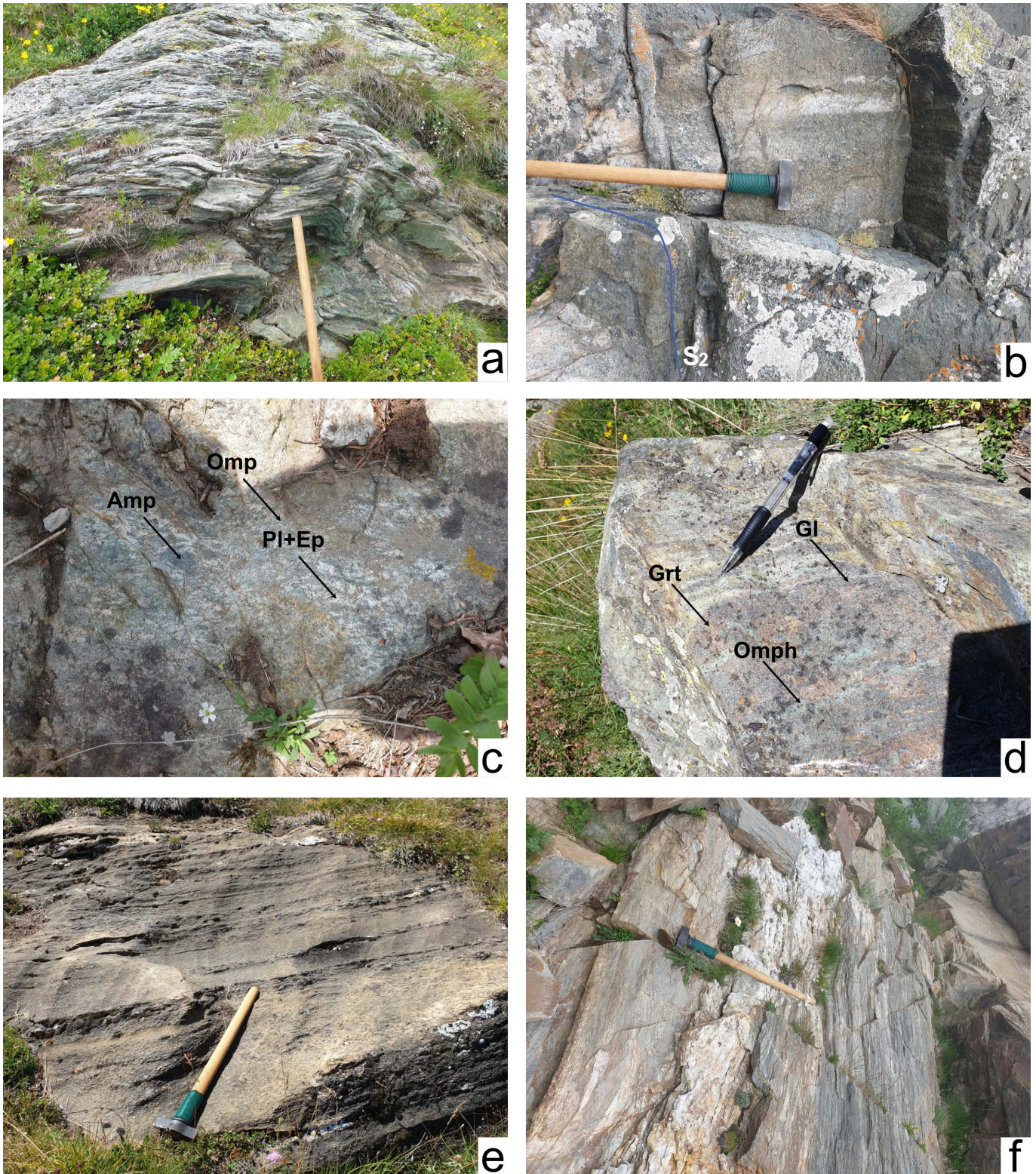
Fig. 2 - Rock types: a) Light green serpentinites with mylonitic foliation. b) Glaucophane and rutile-rich metabasite with coronitic texture on the centre of the picture. On the left side of the picture metabasite with tectonitic texture and S_2 foliation marked by omphacite, amphibole-, and garnet-rich layers that alternate with epidote-, plagioclase-, and minor white mica-rich layers. c) Metagabbro. Green minerals are omphacite (Omp) and amphibole (Amp), and white minerals are plagioclase (Pl) and epidote (Ep). d) Tectonitic eclogite. The reddish to dark blue layers are marked by garnet (Grt) and glaucophane (Gln), and cyanlight green layers are made of omphacite (Omp) partially replaced by green amphibole (Amp), and epidote (Ep). d) Carbonate-rich levels in the calcschists. e) Banded gneisses of the Gran Paradiso Massif. The reader is referred to the PDF article for colour version.

between D_2, D_3, and D_4 folding generated a type 3 interference pattern (Fig. 4d; Ramsay, 1967).

In general, the interference pattern between all generations of folds is not visible given the rather homogeneous topography characterized by a south dipping slope. Isolated interference patterns between PA_2 and PA_3 can be observable in small outcrops of metabasites and calcschists respectively (Fig. 4b, d). However, the similar azimuth of fold axes and
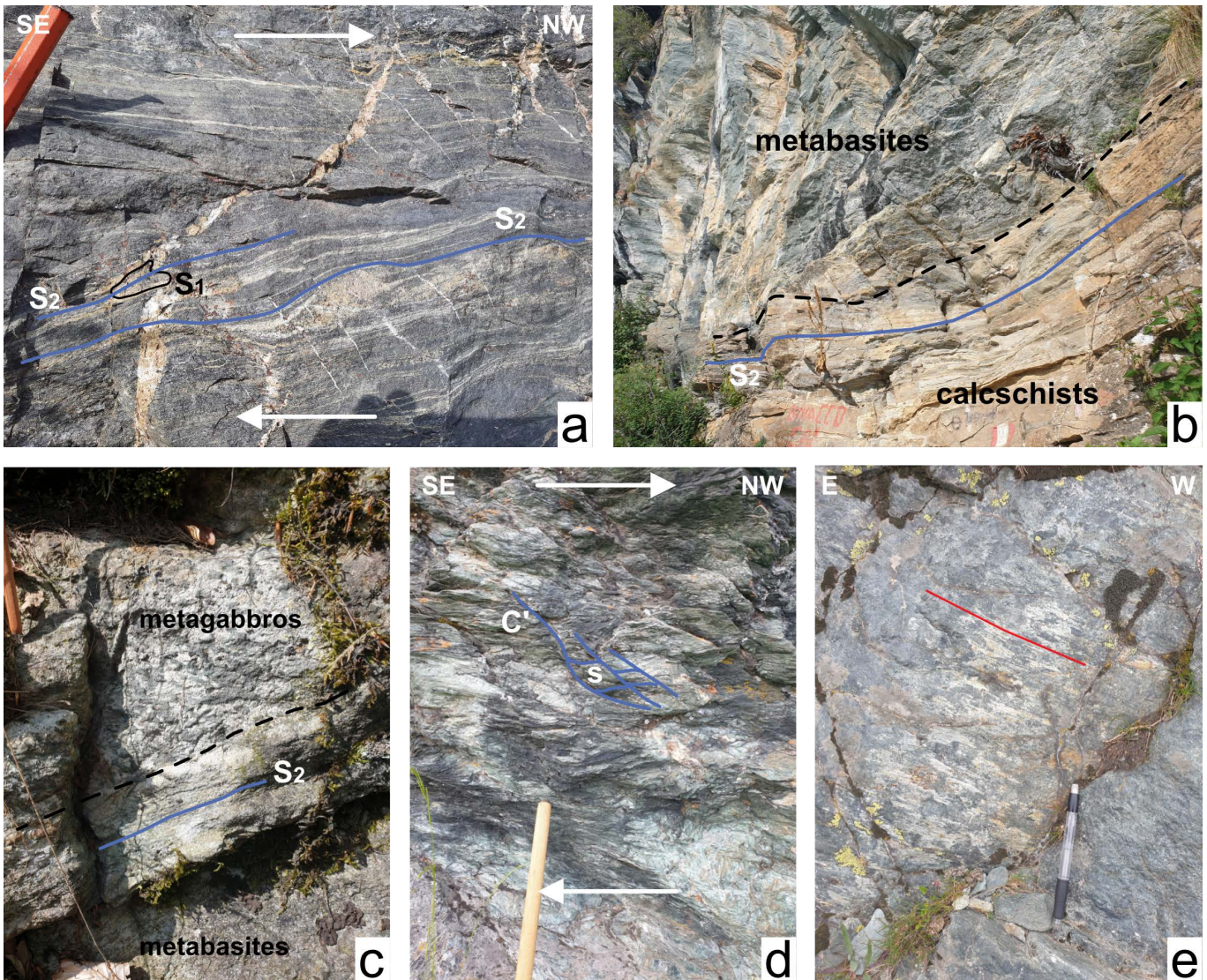
Fig. 3 - Fabrics and structures. a) S_2 mylonitic foliation in metabasites marked by alternating omphacite- and amphibole-rich layers and epidote- and plagio-clase-rich layers. Small lenses containing the S_1 foliation are wrapped by S_2 forming sigmoids and veins filled by epidote are transposed and boudinated resulting in a top-to-right (i.e., NW) sense of shear (white arrows). b) Lithological contact (dashed line) between calcschists and metabasites parallel to the S_2 folia-tion. c) Lithological contact (dashed line) between metagabbros and metabasites parallel to the S_2 foliation. d) S-C' structures in mylonitic serpentinites indi-cating a top-to-right (i.e., NW) sense of shear. e) Quartz-fiber slickensides in the gneiss of Gran Paradiso Massif close to the contact with metaophiolitic rocks.

the different dip of axial planes usually produced a type 3 interference pattern. Similar pattern is generated by PA_3 and PA_4 interference, well observable in serpentinites and calc-schists lenses within metabasites (see localities Parova and Fragne in the geological map, Fig. 1S). Consequently, the lithostratigraphy is strongly affected by the four deformation stages and by the rheology of deformed rocks.

Finally, the last deformation structure mainly developed in a brittle strain field and is characterized by faults and frac-ture systems (Fig. 5f). Those fractures are particularly visible in the gneisses where the intersection between the S_2 foliation and fractures produces isolated rock blocks that usually slide and fall generating large landslide deposits.

MICROSTRUCTURAL ANALYSIS

The principal microstructural characters of the rock types are here presented as a function of the four deformation stag-es investigated in the previous section. In Fig. 6, the rela-

tionships between mineral growth sequence and deformation stages are summarized.

Metabasites

At the microscale, the oldest paragenesis is represented by porphyroclasts of omphacite, garnet, and glaucophane (Fig. 7a), and micro-domains of chlorite and rutile in which the S_1 foliation is locally preserved (Figs 6a and 7b). The second deformation stage (D_2) is associated with the development of the S_2 regional foliation marked by SPO of omphacite, a new generation of glaucophane, epidote, and white mica (Fig. 6a). During post-D_2 stages (D_3 and D_4), the crystallization of green amphibole replacing of omphacite and glaucophane, and chlorite occurred (Fig 6a).

Metagabbros

Relics of clinopyroxene and plagioclase with magmatic texture can be observed at the microscale (Fig. 7c). As for the metabasites, in the metagabbros the first metamorphic imprint is characterized by porphyroclasts of omphacite, garnet, and ru-
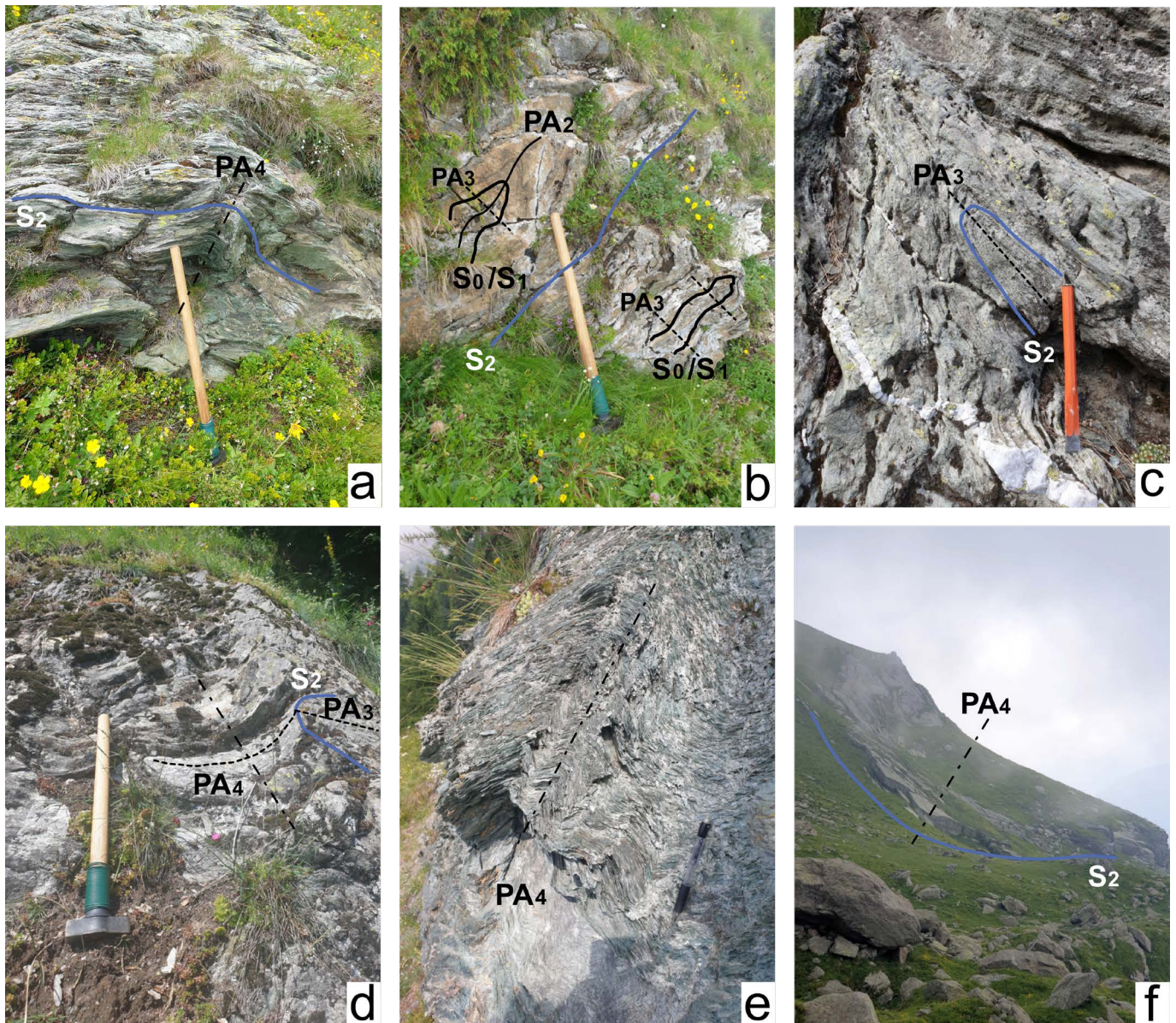
Fig. 4 - a) Highly deformed serpentinite lenses close to the contact with the Gran Paradiso Massif. S_2 axial plane foliation folded by PA_4 axial plane (dashed-dotted trace). b) Relics of PA_2 axial planes and S_2 axial plane foliation deformed by D_3 folds (dashed trace) in calcschists. c) Sub-horizontal PA_3 (dashed black trace) intersecting the S_2 foliation in metabasites. d) PA_3 axial plane (dashed black trace) folded by PA_4 axial plane (dashed-dotted trace) in metabasites. e) Vertical PA_4 axial plane (dashed-dotted trace) with decimetre-scale wavelength in serpentinites. f) Vertical PA_4 axial plane (dashed-dotted trace) with decametre-scale wavelength in metabasites folding S_2 foliation (blue trace).

tile (Fig. 6b). D_1 structures are largely transposed by the successive superposed deformation stages. During D_2, the growth of glaucophane, epidote, white mica, and titanite coronas on rutile occurred (Fig. 6b). The S_2 foliation is marked by alternating omphacite-amphibole-garnet-rich and epidote-rutile-rich layers. During D_3 and D_4, the crystallization of green amphibole replacing glaucophane and omphacite, chlorite, plagioclase, and a new generation of epidote occurred (Figs. 6b and 7d).

Eclogites

The oldest paragenesis is represented by porphyroclasts of omphacite, glaucophane, garnet, and rutile (Fig. 6c). The S_2 foliation is less pervasive than in the other rock types and is characterized by SPO and LPO of glaucophane and epidote (Fig. 7e). During D_2, titanite and ilmenite replaced rutile. As for the previous rock types, during D_3 and D_4, the crystallization of green amphibole replacing glaucophane and ompha-

cite, chlorite, plagioclase, and a new generation of epidote occurred (Figs 6c and 7f).

The contact between metabasites and eclogites is rather parallel to the S_2 foliation and characterized by a reaction rim between the two rocks with larger grain size and different distribution of minerals. The amount of omphacite and garnet increases in the contact zone close to the eclogites and the amount of garnet increases close to the metabasites.

Serpentinites

At the microscale, the serpentinites are strongly foliated with a mylonitic texture. The dominant foliation (S_2), associated to the second deformation stage (D_2), is marked by serpentine, minor chlorite, and opaque (Fig 6d), and present a general S-C' geometry (Fig. 8a). Serpentine-rich layers wrap around serpentine-rich and rare amphibole micro-domains, often characterized by unrooted D_1 folds (Fig. 8b).
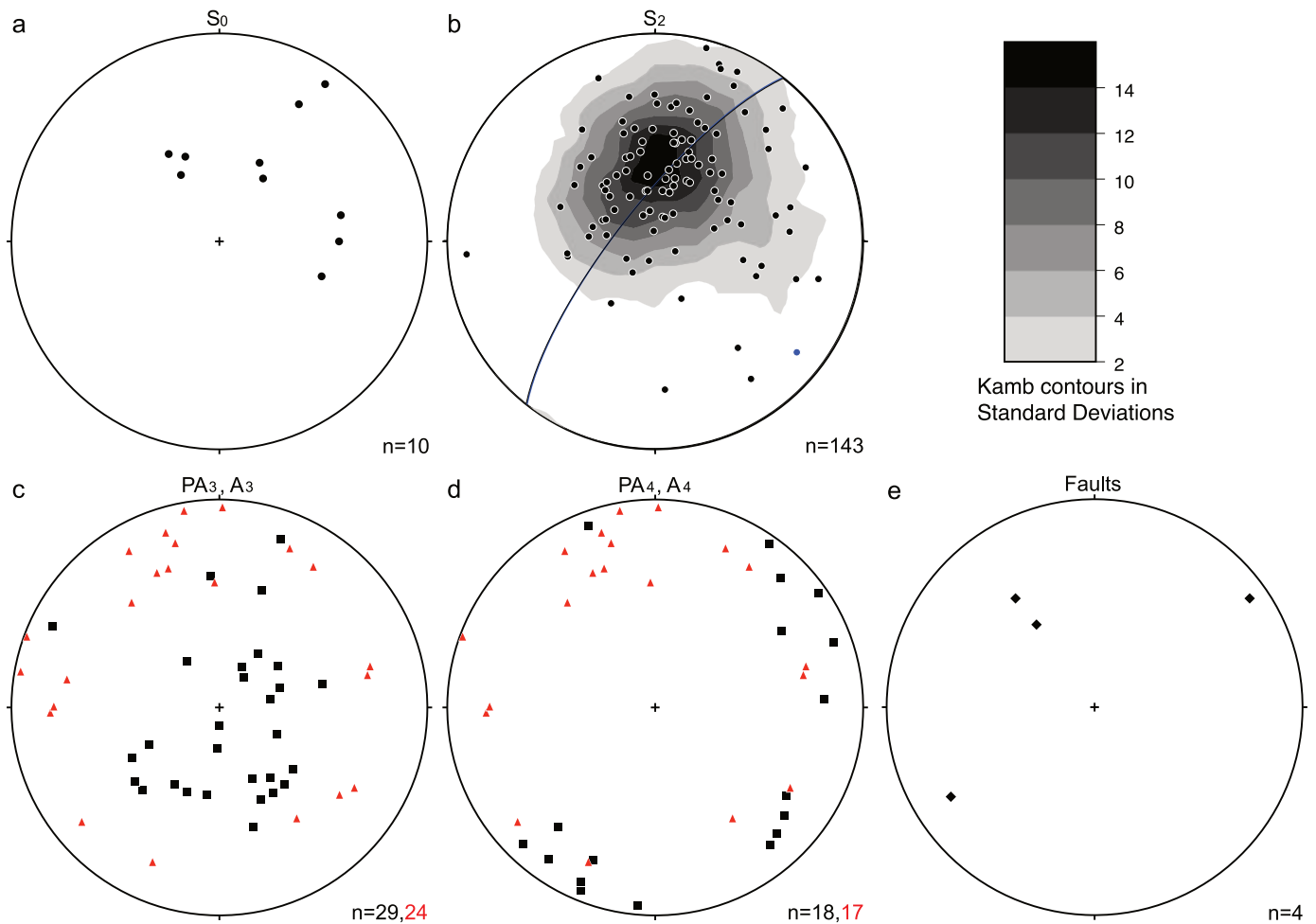
Fig. 5 - Schmid equal area stereographic projections (lower hemisphere) of mesoscopic fabric elements. a) Poles to lithological contact. b) Poles to S_2 foliation and density contours great circle is the best fit plane. c) Poles to PA_3 axial plane (box) and A_3 axis (triangle); d) Poles to PA_4 axial plane (box) and A_4 axis (triangle); f) Poles to fault planes. n - number of measured elements.

Calcschists

These rocks have a dominant S_2 foliation marked by alternating white mica-rich films and calcite- and quartz-rich microlithons (Figs 6e and 8c, d). White mica-rich films are discontinuous with a mainly wriggly shape (Fig. 8d). During D_3 and D_4 deformation stages, a new generation of white mica with larger grain size, opaque, and tourmaline crystals formed (Fig. 6e) crosscutting the S_2 foliation. The contact between calcschists and metabasites and serpentinites is rather parallel to S_2 and is marked by centimetre-sized grains of calcite and serpentine.

Gneisses

The oldest paragenesis in these rocks is represented by relics of quartz, plagioclase, and garnet detectable in microdomains (Fig. 6f) that are wrapped by the dominant S_2 foliation (Fig. 8e). S_2 is a spaced foliation characterized by white mica-rich films and quartz- and plagioclase-rich microlithons (Fig. 6f). In quartz-rich portions of the rock, S_2 is marked by SPO of quartz with discontinuous and irregular white mica-rich films. Locally, a S-C' geometry is visible in white mica-rich portions of the rock (Fig. 8f). During D_3 and D_4, a new generation of white mica and opaque formed (Fig, 6f).

TECTONIC EVOLUTION

The lithological and structural analyses synthetized in this work allows a better definition of the tectonic evolution of the Lower Piemonte Zone metaophiolites in the Val d'Ala area. In the ophiolites a complete but transposed lithostratigraphy of the oceanic lithosphere occurs, as already indicated for neighbouring areas (Spalla et al., 1983; Leardi et al., 1984; Assanelli et al., 2020; De Togni et al., 2021; Herviou et al., 2022). Serpentinites clearly represent a part of hydrated oceanic. Metabasites have a MORB signature irrespective of their textures (Leardi et al., 1984) and are supposed to be metamorphosed basalts (Leardi and Rossetti, 1985). In the study area, metagabbros are intruded within metabasites and derived from original Mg-gabbros while, on the basis of texture and chemistry, eclogites are supposed to be originated from FeTi-gabbros (Leardi et al., 1984; Leardi and Rossetti, 1985). Calcschists represent metamorphosed calcareous and silico-clastic covers of the metaophiolite (Sandrone et al., 1986). This lithostragraphy is almost coherent with that of other metaophiolites of the Western Alps variably affected by Alpine deformation and metamorphism and consists of serpentinized peridotites covered by basaltic lavas and calc-

a METABASITES

Mineral	M1/D1	D2	D3/D4
Cpx	Omph	Omph	
Amp	Gln	Gln	green Amph
Grt			
Ep			
Chl			
Rt			
Op		Mag	Mag
Wm			
Qz			
Cc			

b METAGABBROS

Mineral	MAGM	M1/D1	D2	D3/D4
Cpx	Magm	Omph	Omph	
Amp			Gln	green Amph
Grt				
Ep				
Chl				
Rt				
Pl				
Ttn				
Wm				
Cc				

c ECLOGITES

Mineral	D1	D2	D3/D4
Cpx	Omph	Omph	
Grt			
Rt			
Amp	Gln	Gln	green Amph
Ep			
Op		Mag	Mag
Chl			
Ttn/Ilm		Ttn	Ilm
Qz			
Pl			

d SERPENTINITES

Mineral	D1	D2	D3/D4
Srp			
Op		Mag	
Amp			
Chl			

f GNEISSES

Mineral	D1	D2	D3/D4
Qz			
Pl			
Grt			
Wm			
Op			

e CALCSCHISTS

Mineral	D1	D2	D3/D4
Cc			
Qz			
Wm			
Op			
Tur			

Fig. 6 - Blastesis vs deformation (D) and metamorphism (M) diagrams illustrating the relationships between mineral growth sequence and deformation stages for the six investigated rock types.

silicate sediments (e.g., Lombardo et al., 1978; Lagabrielle and Polino, 1988; Schwartz et al., 2000; Li et al., 2004b; Bucher et al., 2005; Zanoni et al., 2016; Balestro et al., 2019; Luoni et al., 2019; Agard, 2021). On the contrary to what observed in Val d'Ala, in the other ophiolites of the Western Alps metagabbros (Fe- and Mg-rich) are usually found as intrusive bodies within peridotites (Balestro et al., 2019), with the exception of some areas in Zermatt-Saas zone (Gilio et al., 2019; Bucher et al., 2020). These ophiolites were part of the Liguria-Piemonte Ocean interpreted as generated by slow to ultraslow spreading ridge (Lemoine and Trümpy, 1987;

Michard et al., 1996; Lavier and Manatschal, 2006; Saccani et al., 2015). In the area of survey gneiss of Gran Paradiso Massif are in principal paragneiss although some lenses of orthogneiss have been described more eastward by Caso et al. (2021).

Eclogites, coronitic metagabbros, and metabasites recorded the oldest metamorphic stage during D_1 characterized by omphacite, garnet, rutile and glaucophane. This HP mineral assemblage results in minimum PT conditions of 1.3 GPa and 450-460°C (Sandrone et al., 1986). Eclogite-facies metamorphic conditions with significantly higher pressure (2.1-2.5 GPa)
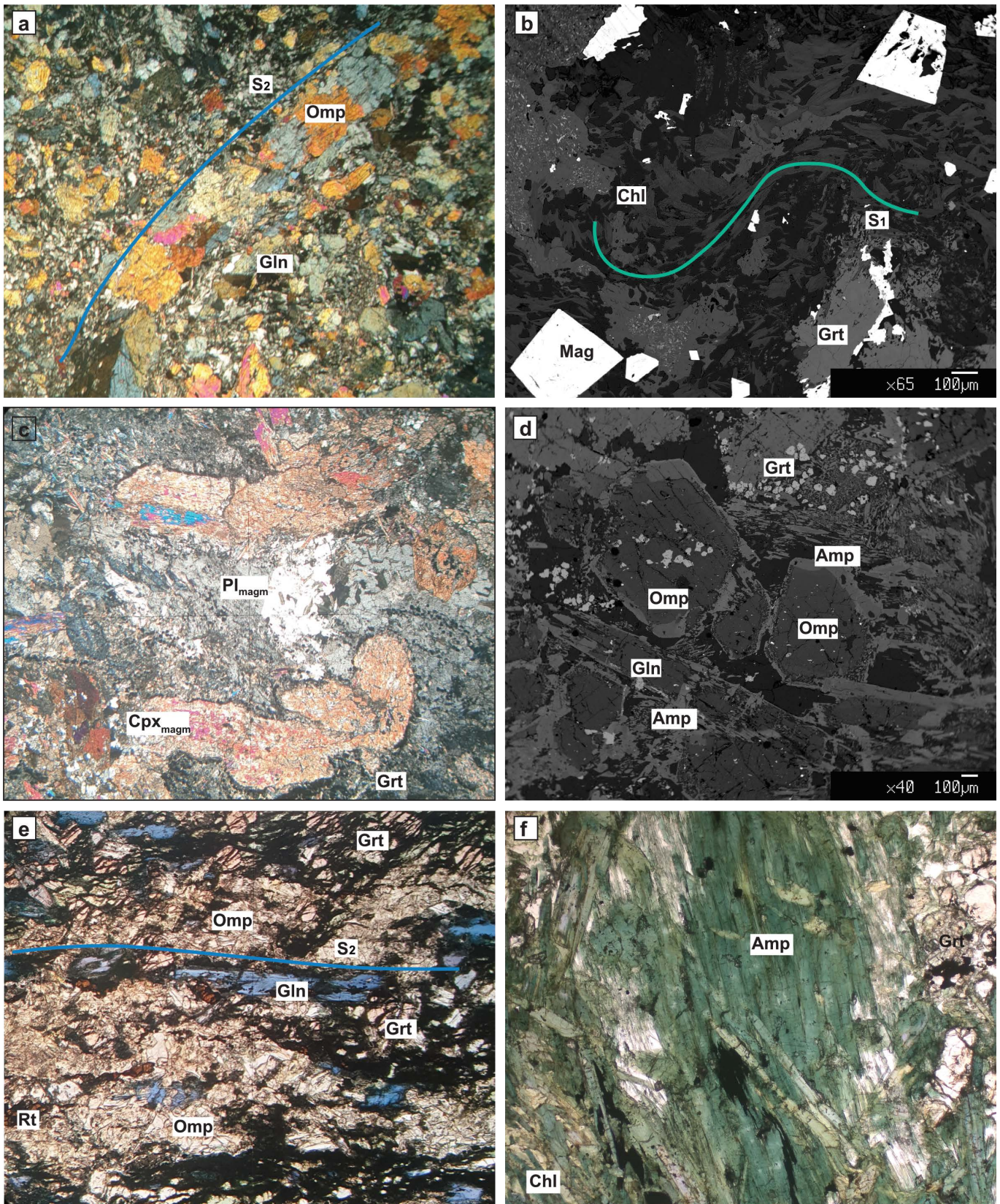
Fig. 7 - Microstructures in metabasites (a, b), metagabbros (c, d), and eclogite (e, f). a) Crossed polar image of omphacite (Omp) porphyroclasts wrapped by the S_2 foliation in metabasites. The clinopyroxene porphyroclasts are partially replaced by green amphibole (Amp). Long Side Picture (LSP) = 6 mm. b) Back-Scattered Electron (BSE) image of chlorite-bearing micro-domains characterized by relict S_1 foliation in metabasites. c) Crossed polar image of relicts of magmatic clinopyroxene (Cpx_{magm}) and plagioclase (Pl_{magm}) in coronitic metagabbros. LPS = 6 mm. d) Back-Scattered Electron (BSE) image of green amphibole replacing omphacite (Omp) and glaucophane (Gln) in metagabbros. e) SPO and LPO of glaucophane (Gln) marking the S_2 foliation that wrapped omphacite (Omp), garnet (Grt), and rutile (Rt) porphyroclasts in eclogites. LPS = 6 mm. f) Green amphiboles (Amp2) replacing glaucophane (Gln) and chlorite (Chl) in eclogites. LSP = 3.3 mm.
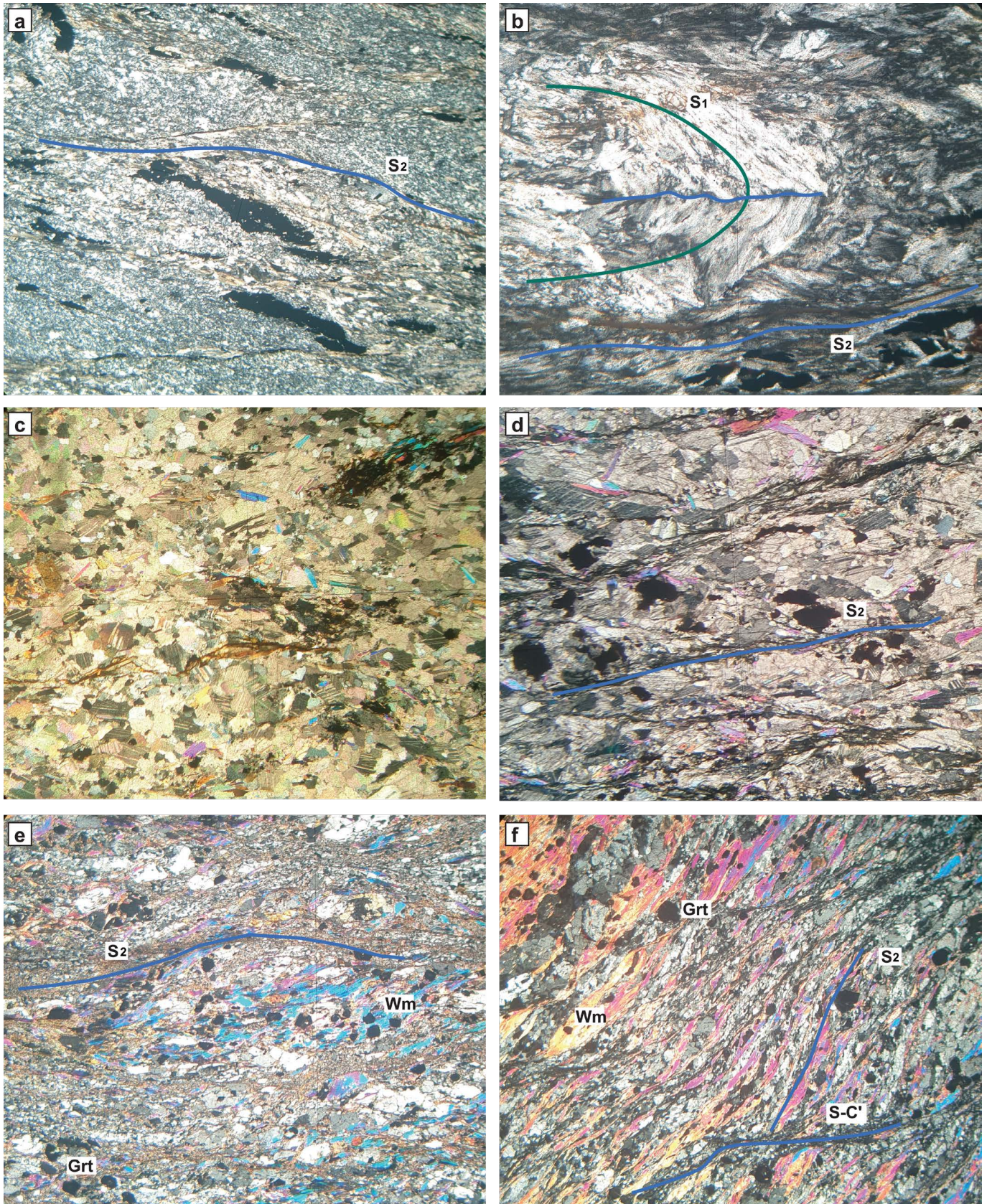
Fig. 8 - Microstructures in serpentinites (a,b), calcschists (c,d), and gneisses (e,f). a) S_2 foliation marked by SPO of serpentine in serpentinites. Long Side Picture (LSP) = 6 mm. b) Serpentine-rich micro-domain characterized by unrooted D_1 fold and wrapped by the S_2 foliation in serpentinites. LSP = 3 mm. c) Crossed polar image of calcite-rich layer in calcschists. LSP = 6 mm. d) Crossed polar image of the S_2 foliation marked by alternating white-mica-rich films and calcite- and quartz-rich microlithons in calcschists. LSP = 6 mm. e) Crossed polar image of quartz-, plagioclase-, and garnet-rich micro-domains wrapped by the dominant S_2 foliation in gneisses. LSP = 6 mm. f) Crossed polar image of S-C' geometry in white mica-rich portions (Wm) in gneisses. LSP = 6 mm.

are also estimated from the metaophiolites in neighbouring areas (Susa Valley - Ghignone et al., 2021a; Stura di Viù Valley - Balestro et al., 2009; De Togni et al., 2021) and dated between 41 and 47 Ma (Ghignone et al., 2021b). These relict minerals occur as porphyroclasts or defining SPO in the regional S_2 foliation (during D_2) marked by glaucophane and epidote in the metabasites and metagabbros, serpentine in the serpentinites, and carbonate + quartz ± garnet ± epidote-rich lithons and with mica + chlorite-rich films in the calcschists. The S_2 foliation also developed within the gneiss of the Gran Paradiso Massif and is parallel to the lithological contacts. Therefore, in this area, the present-day structure of lithological boundaries is generated during the D_2 deformation stage as well as the coupling between the Lower Piemonte Zone and the Gran Paradiso Massif. The mineral assemblages formed during D_2 suggests a re-equilibration under blueschist-facies conditions. The S_2 foliation in Susa Valley that would represent the first metamorphic event after the pressure peak, has been dated at 37 Ma. However, in this case S_2 developed under greenschist facies conditions and therefore cannot be fully representative of the D_2 event in Val d'Ala.

Locally green amphibole, chlorite and new plagioclase replace omphacite and glaucophane that suggest a re-equilibration under lower pressure and temperature than D_2 conditions. This mineral assemblage is clearly successive to D_2, but it is not clear in which of the following stages is formed. Three successive folding stages occurred with variable wavelengths and geometries as a function of the deformed lithology. D_3 is characterized by a mainly sub-horizontal fold plane and D_4 by a sub-vertical fold plane. Other data and, possibly, a numerical modelling would be necessary to propose a non-speculative, tectonic evolution of these units, but possible evolutionary models to refer to in the geodynamic frame of the Western Alps, could be those proposed in literature by Assanelli et al. (2020), Agard (2021), and Ghignone et al. (2021b).

Four ductile deformative phases have been describe by Caso et al. (2021) and consist of three folding events (our D_2, D_3, and D_4) with the development a pervasive axial plane foliation (our S_2) during the first event, and a discontinuous spaced crenulation cleavage within serpentinites during D_3. A discontinuous S_1 foliation has been also observed within metabasites. The metamorphic associations reported by Caso et al. (2021) are comparable to those described in this work suggesting similar tectonic evolution. Four ductile deformative phases have been also observed in the metaophiolite of the southern Upper Viù Valley, all associated with the development of axial plane foliations (De Togni et al., 2023). In analogy with the Ala Valley, the S_2 foliation is the more pervasive structure in the Upper Viù Valley, PA_3 are sub-horizontal, and PA_4 has a high angle dip.

CONCLUSION

The geological and structural study of the Val d'Ala metaophiolite complex evidenced that serpentinites and metabasites are the dominant rocks and are deformed together with hectometre-sized calcschist bodies, metre to decametre-sized metagabbro bodies, and some metre-sized eclogite lenses. Four groups of superposed structures have been recognized. The D_1 relict fabrics occur in eclogites, metagabbros, and metabasites and are marked by omphacite, garnet, rutile, and glaucophane. The mineral assemblage suggests a metamorphic peak under eclogite-facies conditions. The D_2 structures consist of isoclinal folds and the S_2 axial plane fo-

liation is marked by glaucophane and epidote in the metabasites, metagabbros, and eclogites, serpentine and chlorite in the serpentinites, carbonate, quartz, white mica in the calcschists and quartz, plagioclase, and white mica in the gneisses. The mineral assemblages suggest a re-equilibration under blueschist-facies conditions. The lithological boundaries and the tectonic contact between the Piemonte Zone metaophiolite and the gneisses of the Gran Paradiso Massif is parallel to S_2. D_3 structures consists of a fold system with sub-horizontal axial plane (PA_3) and axis (A_3) and D_4 fabric consists of isoclinal to open folds with sub-vertical dipping axial plane (PA_4) and sub-horizontal axis (A_4). From D_3 local replacement of omphacite and glaucophane with green amphibole, chlorite and plagioclase can be observed.

The general evolution can be summarized as the subduction of part of the lithosphere belonging to the Ligure-Piemontese Ocean up to eclogite-facies conditions recorded during D_1. During D_2 a re-equilibration in blueschists-facies conditions occurred and the ophiolites of the Lower Piemonte Zone and the gneisses of the Gran Paradiso Massif coupled together. Then, the tectono-metamorphic unit exhumed and underwent up to 2 successive ductile deformation stages (D_3 and D_4).

REFERENCES

Agard P., 2021. Subduction of oceanic lithosphere in the Alps: Selective and archetypal from (slow-spreading) oceans. Earth-Sci. Rev., 214: 1-34. https://doi.org/10.1016/j.earscirev.2021.103517

Agard P. and Handy M.R., 2021. Ocean subduction dynamics in the Alps. Elements, 17; 9-16. https://doi.org/10.2138/gselements.17.1.9

Allmendinger R.W., Cardozo N.C. and Fisher D., 2013. Structural geology algorithms: Vectors and Tensors. Cambridge Univ. Press, Cambridge

Angiboust S., Agard P., Jolivet L. and Beyssac O., 2009. The Zermatt-Saas ophiolite: The largest (60-km wide) and deepest (c. 70-80km) continuous slice of oceanic lithosphere detached from a subduction zone? Terra Nova, 21: 171-180. https://doi.org/10.1111/j.1365-3121.2009.00870.x

Assanelli M., Luoni P., Rebay G., Roda M. and Spalla, M.I., 2020. Tectono-metamorphic evolution of serpentinites from Lanzo Valleys Subduction Complex (Piemonte-Sesia-Lanzo Zone boundary, Western Italian Alps). Minerals, 10: 1-39. https://doi.org/10.3390/min10110985

Babist J., Handy M.R., Konrad-Schmolke M. and Hammerschmidt K., 2006. Precollisional, multistage exhumation of subducted continental crust: The Sesia Zone, Western Alps. Tectonics, 25. https://doi.org/10.1029/2005TC001927

Balestro G., Cadoppi P., Perrone G. and Tallone S., 2009. Tectonic evolution along the Col del Lis-Trana Deformation Zone (internal Western Alps). Ital. J. Geosci., 128: 331-339. https://doi.org/10.3301/IJG.2009.128.2.331

Balestro G., Festa A. and Dilek Y., 2019. Structural architecture of the Western Alpine ophiolites, and the Jurassic seafloor spreading tectonics of the Alpine Tethys. J. Geol. Soc., 176: 913-930. https://doi.org/10.1144/jgs2018-099

Barnicoat, A.C., Fry, N., 1986. High -pressure metamorphism of the Zermatt-Sass ophiolite, Switzerland. Journal of the Geological Society 143, 607–618.

Bearth P., 1967. Die ophiolite der Zone von Zermatt-Sass Fee. Beitrag Geologische Karte Schweitz, 132: 1-130.

Bearth P. and Schwander H., 1981. The post-Triassic sediments of the ophiolite zone Zermatt-Saas Fee and the associated manganese mineralizations. Ecl. Geol. Helv., 74: 189-205.

Bertrand J.-M., Paquette J.-L. and Guillot F., 2005. Permian zircon U–Pb ages in the Gran Paradiso massif: revisiting post-Variscan events in the Western Alps. Schweiz. Miner. Petrogr. Mitt., 85: 15-29.

Bigi G., Cosentino D., Parotto M., Sartori R. and Sandone P., 1990. Structural Model of Italy and gravity map. Scale 1: 500.000, Sheets 1-9 C.N.R., Progetto finalizzato Geodinamica. Quaderni de «La Ricerca Scientifica», 114.

Borghi A., Compagnoni R. and Sandrone R., 1996. Composite P-T paths in the Internal Penninic Massifs of the western Alps : petrological constraints to their thermo-mechanical evolution. Ecl. Geol. Helv., 89: 345-367. https://doi.org/10.5169/seals-167905

Bousquet R., Oberhansli R., Goffé B., Wiederkehr M., Koller F., Schmid S.M., Schuster R., Engi M., Berger A. and Martinotti G., 2008. Metamorphism of metasediment at the scale of an orogen: a key to the Tertiary geodynamic evolution of the Alps. Geol. Soc. London Spec. Publ., 298: 393-411. https://doi.org/10.1144/SP298.18

Bucher K. and Grapes R., 2009. The eclogite-facies Allalin gabbro of the Zermatt-Saas ophiolite, Western Alps: A record of subduction zone hydration. J. Petrol., 50: 1405–1442. https://doi.org/10.1093/petrology/egp035

Bucher K. and Stober I., 2021. Metamorphic gabbro and basalt in ophiolitic and continental nappes of the Zermatt region (Western Alps). Swiss J. Geosci., 114: 12. https://doi.org/10.1186/s00015-021-00390-w

Bucher K., Fazis Y., de Capitani C. and Grapes R., 2005. Blueschists, eclogites, and decompression assemblages of the Zermatt-Saas ophiolite: High-pressure metamorphism of subducted Tethys lithosphere. Am. Miner., 90: 821-835. https://doi.org/10.2138/am.2005.1718

Bucher K., Weisenberger T.B., Weber S., Klemm O. and Corfu F., 2020. The Theodul Glacier Unit, a slab of pre-Alpine rocks in the Alpine meta-ophiolite of Zermatt-Saas, Western Alps. Swiss J. Geosci., 113: 1. https://doi.org/10.1186/s00015-020-00354-6

Callegari E., Compagnoni R. and Dal Piaz G.V., 1969. Relitti di strutture intrusive erciniche e scisti a sillimanite nel Massiccio del Gran Paradiso. Boll. Soc. Geol. It., 88: 59-69.

Cantù M., Spaggiari L., Zucali M., Zanoni D. and Spalla M.I., 2016. Structural analysis of a subduction-related contact in southern Sesia-Lanzo Zone (Austroalpine Domain, Italian Western Alps). J. Maps, 12: 22-35. https://doi.org/10.1080/17445647.2016.1155925

Cardozo N. and Allmendinger R.W., 2013. Spherical projections with OSXStereonet. Comput. Geosci., 51: 193-205. https://doi.org/10.1016/j.cageo.2012.07.021

Caron J.M., Polino R., Pognante U., Lombardo B., Lardeaux L.M., Lagabrielle Y., Gosso G. and Allenbach B., 1984. Ou sont les sutures majeures dans les Alpes internes? (transversale Briançon-Torino). Mem. Soc. Geol. It., 29: 71-78.

Caso F., Nerone S., Petroccia A. and Bonasera M., 2021. Geology of the southern Gran Paradiso Massif and Lower Piedmont Zone contact area (middle Ala Valley, Western Alps, Italy). J. Maps,, 17: 237-246. https://doi.org/10.1080/17445647.2021.1911869

Castelli D., Rolfo F., Groppo C. and Compagnoni R., 2007. Impure marbles from the UHP Brossasco-Isasca Unit (Dora-Maira Massif, Western Alps): evidence for Alpine equilibration in the diamond stability field and evaluation of the X(CO 2) fluid evolution. J. Metam. Geol., 25: 587-603. https://doi.org/10.1111/j.1525-1314.2007.00716.x

Chopin C., Henry C. and Michard A., 1991. Geology and petrology of the coesite-bearing terrain, Dora Maira massif, Western Alps. Eur. J. Miner., 3: 263-292. https://doi.org/10.1127/ejm/3/2/0263

Compagnoni R. and Prato R., 1969. Paramorfosi di cianite e sillimanite in scisti pregranitici del massiccio del Gran Paradiso. Boll. Soc. Geol. It., 88: 537-549.

Compagnoni R., Elter G. and Lombardo B., 1974. Eterogeneità stratigrafica del complesso degli "Gneiss Minuti" del massiccio cristallino del Gran Paradiso. Mem. Soc. Geol. It., 13: 227-239.

Dal Piaz G.V., 1988. Revised setting of the Piedmont zone in the northern Aosta Valley, Western Alps. Ofioliti, 13: 157-162.

Dal Piaz G.V., 1966. Gneiss ghiandoni, marmi ed anfiboliti antiche del ricoprimento Monte Rosa nell'alta Valle d'Ayas. Boll. Soc. Geol. It., 85: 103-132.

Dal Piaz G.V., Di Battistini G., Kienast J.R. and Venturelli G., 1979. Manganiferous quartzitic schists of the Piemonte ophiolite nappe in the Valsesia-Valtournanche area (Italian Western Alps). Mem. Sci. Geol., 32: 1-24.

Dal Piaz G.V. and Ernst W.G., 1978. Areal geology and petrology of eclogites and associated metabasites of the Piemonte ophiolite nappe, Breuil - St. Jacques area, Italian Western Alps. Tectonophysics, 51: 99-126. https://doi.org/10.1016/0040-1951(78)90053-7

Dal Piaz G.V., Venturelli G., Spadea P. and Di Battistini G., 1981. Geochemicl features of metabasalts and metagabbros from the Piemonte ophiolite nappe, Italian Western Alps. N. Jahrb. Miner. Abhandl., 142: 248–269.

Dal Piaz G. V., 2010. The Italian Alps: a journey across two centuries of Alpine geology. In: M. Beltrando, A. Peccerillo, M. Mattei, S. Conticelli and C. Doglioni (Eds.), J. Virtual Expl., 36, 8. https://doi.org/10.3809/jvirtex.2010.00234

Dal Piaz G.V., Hunziker J.C. and Martinotti G., 1972. La Zona Sesia - Lanzo e l'evoluzione tettonico-metamorfica delle Alpi Nordoccidentali interne. Mem. Soc. Geol. It., 11,: 433-460.

de Meyer C.M.C., Baumgartner L.P., Beard B.L. and Johnson C.M., 2014. Rb-Sr ages from phengite inclusions in garnets from high pressure rocks of the Swiss Western Alps. Earth Planet. Sci. Lett., 395: 205-216. https://doi.org/10.1016/j.epsl.2014.03.050

De Togni M., Gattiglio M., Balestro G. and Roà M., 2023. Alpine structural evolution of the Internal Piedmont Zone in the Upper Viù Valley (Lanzo Valleys Ophiolite, Western Alps). Rend. Online Soc. Geol. It., 60: 1-8. https://doi.org/10.3301/ROL.2023.27

De Togni M., Gattiglio M., Ghignone S. and Festa A., 2021. Pre-Alpine tectono-stratigraphic reconstruction of the Jurassic Tethys in the High-Pressure Internal Piedmont Zone (Stura di Viù Valley, Western Alps). Mineral, 11: 361. https://doi.org/10.3390/min11040361

Diella V., Bocchio R., Marinoni N., Caucia F., Spalla M.I., Adamo I., Langone A. and Mancini L., 2019. Garnets from Val d'Ala rodingites, Piedmont, Italy: An Investigation of their gemological, spectroscopic and crystal chemical properties. Minerals, 9: 728. https://doi.org/10.3390/min9120728

Dragovic, B., Angiboust, S., Tappa, M.J., 2020. Petrochronological close-up on the thermal structure of a paleo-subduction zone (W. Alps). Earth and Planetary Science Letters 547, 1–12. https://doi.org/10.1016/j.epsl.2020.116446

Escher A., Hunziker J.C., Marthaler M., Masson H., Sartori M. and Steck A., 1997. Geologic framework and structural evolution of the Western Swiss-Italian Alps. In: O.A. Pfiffner, P. Lehner, P.Z. Heitzmann, S., Mueller and Steck A. (Eds.), Deep structure of the Swiss Alps: Results from NRP 20. Birkhäuser-Verlag, Basel (Swissland), 205-221.

Fontana E., Panseri M. and Tartarotti P., 2008. Oceanic relict textures in the Mount Avic Serpentinites, Western Alps. Ofioliti 33: 105-118. https://doi.org/10.4454/ofioliti.v33i2.367

Fontana E., Tartarotti P., Panseri M. and Buscemi S., 2015. Geological map of the Mount Avic massif (Western Alps Ophiolites). J. Maps, 11: 126-135. https://doi.org/10.1080/17445647.2014.959567

Frezzotti M.L., Selverstone J., Sharp Z.D. and Compagnoni R., 2011. Carbonate dissolution during subduction revealed by diamond-bearing rocks from the Alps. Nature Geosci., 4: 703-706. https://doi.org/10.1038/ngeo1246

Gabudianu Radulescu I., Compagnoni R. and Lombardo B., 2011. Polymetamorphic history of a relict Permian hornfels from the central Gran Paradiso Massif (Western Alps, Italy): a microstructural and thermodynamic modelling study. J. Metam. Geol., 29: 851-874. https://doi.org/10.1111/j.1525-1314.2011.00943.x

Gasco I., Borghi A. and Gattiglio M., 2011a. P–T Alpine metamorphic evolution of the Monte Rosa nappe along the Piedmont Zone boundary (Gressoney Valley, NW Italy). Lithos, 127: 336-353. https://doi.org/10.1016/j.lithos.2011.09.007

Gasco I., Borghi A. and Gattiglio M., 2010. Metamorphic evolution of the Gran Paradiso Massif: A case study of an eclogitic metagabbro and a polymetamorphic glaucophane–garnet micaschist. Lithos, 115: 101-120. https://doi.org/10.1016/j.lithos.2009.11.009

Gasco I., Gattiglio M. and Borghi A., 2013. Review of metamorphic and kinematic data from Internal Crystalline Massifs (Western Alps): PTt paths and exhumation history. J. Geodyn., 63: 1-19. https://doi.org/10.1016/j.jog.2012.09.006

Gasco I., Gattiglio M. and Borghi A., 2011b. Lithostratigraphic setting and P-T metamorphic evolution for the Dora Maira Massif along the Piedmont Zone boundary (middle Susa Valley, NW Alps). Intern. J. Earth Sci., 100: 1065-1085. https://doi.org/10.1007/s00531-011-0640-8

Ghignone S., Borghi A., Balestro G., Castelli D., Gattiglio M. and Groppo C., 2021a. HP tectono-metamorphic evolution of the Internal Piedmont Zone in Susa Valley (Western Alps): New petrologic insight from garnet+chloritoid-bearing micaschists and Fe–Ti metagabbro. J. Metam. Geol., 39: 391-416. https://doi.org/10.1111/jmg.12574

Ghignone S., Sudo M., Balestro G., Borghi A., Gattiglio M., Ferrero S. and van Schijndel V., 2021b. Timing of exhumation of meta-ophiolite units in the Western Alps: New tectonic implications from $^{40}Ar/^{39}Ar$ white mica ages from Piedmont Zone (Susa Valley). Lithos, 404-405: 106443. https://doi.org/10.1016/j.lithos.2021.106443

Gilio M., Scambelluri M., Agostini S., Godard M., Peters D. and Pettke T., 2019. Petrology and geochemistry of serpentinites associated with the Ultra-High Pressure Lago di Cignana Unit (Italian Western Alps). J. Petrol., 60: 1229-1262. https://doi.org/10.1093/petrology/egz030

Gosso G., Rebay G., Roda M., Spalla M.I., Tarallo M., Zanoni D. and Zucali M., 2015. Taking advantage of petrostructural heterogeneities in subduction- collisional orogens, and effect on the scale of analysis. Periodico Di Mineralogia 84, 779–825. https://doi.org/10.2451/2015PM0452

Gouzu C., Yagi K., Thanh N.X., Itaya T. and Compagnoni R., 2016. White mica K-Ar geochronology of HP–UHP units in the Lago di Cignana area, western Alps, Italy: Tectonic implications for exhumation. Lithos, 248-251: 109-118. https://doi.org/10.1016/j.lithos.2016.01.015

Groppo C., Beltrando M. and Compagnoni R., 2009. The P-T path of the ultra-high pressure Lago Di Cignana and adjoining high-pressure meta-ophiolitic units: Insights into the evolution of the subducting Tethyan slab. J. Metam. Geol., 27: 207-231. https://doi.org/10.1111/j.1525-1314.2009.00814.x

Groppo C. and Compagnoni R., 2007. Metamorphic veins from the serpentinites of the Piemonte Zone, Western Alps, Italy: A review. Per. Miner,, 76: 127-153. https://doi.org/10.2451/2007PM0021

Herviou C., Agard P., Plunder A., Mendes K., Verlaguet A., Deldicque D. and Cubas N., 2022. Subducted fragments of the Liguro-Piemont Ocean, Western Alps: Spatial correlations and off-scraping mechanisms during subduction. Tectonophysics, 827: 229267. https://doi.org/10.1016/j.tecto.2022.229267

Kienast J.R., 1983. Le métamorphisme de haute pression et basse température (Eclogites et Schistes Bleus): Données nouvelles sur la pétrologie de la croûte océanique subductée et des sédiments associés. PhD Thesis, Univ. Paris VI.

Lagabrielle Y. and Polino R., 1988. Un schéma structural du domaine des Schistes Lustrés ophiolitifères au nord ouest du massif du Mont Viso (Alpes Sud Occidentales) et ses implications. C.R. Acad. Sci. Paris, 306: 921-928.

Lapen T., Johnson C., Baumgartner L., Piaz,G., Skora S. and Beard B., 2007. Coupling of oceanic and continental crust during Eocene eclogite-facies metamorphism: evidence from the Monte Rosa nappe, western Alps. Contrib. Miner. Petrol., 153: 139-157.

Lapen T.J., Johnson C.M., Baumgartner L.P., Mahlen N.J., Beard B.L. and Amato J.M., 2003. Burial rates during prograde metamorphism of an ultra-high-pressure terrane: an example from Lago di Cignana, western Alps, Italy. Earth Planet. Sci. Lett., 215: 57-72. https://doi.org/10.1016/S0012-821X(03)00455-2

Lardeaux J.-M., 2014. Deciphering orogeny: a metamorphic perspective. Examples from European Alpine and Variscan belts: Part I: Alpine metamorphism in the Western Alps. A review. Bull. Soc. Gèol. Fr., 185: 93-114. https://doi.org/10.2113/gssgfbull.185.2.93

Lavier L.L. and Manatschal G., 2006. A mechanism to thin the continental lithosphere at magma-poor margins. Nature, 440: 324-328.

Le Bayon B., Pitra P., Ballèvre M. and Bohn M., 2006. Reconstructing P-T paths during continental collision using multi-stage garnet (Gran Paradiso nappe, Western Alps). J. Metam. Geol., 24: 477-496. https://doi.org/10.1111/j.1525-1314.2006.00649.x

Le Bayon R., de Capitani C., Chopin C. and Frey M., 2000. Modelling of the sequential evolution of whiteschist assemblages: HP in the Monte Rosa (Western Alps). Eur. J. Miner., 12: 111.

Le Bayon, R., de Capitani, C. and Frey M., 2006. Modelling phase-assemblage diagrams for magnesian metapelites in the system K_2O-FeO-MgO-Al_2O_3-SiO_2-H_2O: geodynamic consequences for the Monte Rosa nappe, Western Alps. Contrib. Miner. Petrol., 151: 395-412. https://doi.org/10.1007/s00410-006-0067-6

Leardi L. and Rossetti P., 1985. Caratteri geologici e petrografici delle metaofioliti della Val d'Ala (Valli di Lanzo, Alpi Graie). Boll. Ass. Miner. Subalp., 22: 422441.

Leardi L., Rossetti P. and Compagnoni R., 1984. Geochemical study of a metamorphic ophiolite sequence from the Val d'Ala di Lanzo (internal Piemontese Zone, Graian Alps, Italy). Mem. Soc. Geol. It., 29: 93-105.

Lemoine M. and Trümpy R., 1987. Pre-oceanic rifting in the Alps. Tectonophysics, 133: 305-320. https://doi.org/10.1016/0040-1951(87)90272-1

Li X.-H., Faure M., Lin W. and Manatschal G., 2013. New isotopic constraints on age and magma genesis of an embryonic oceanic crust: The Chenaillet Ophiolite in the Western Alps. Lithos, 160-161: 283-291. https://doi.org/10.1016/j.lithos.2012.12.016

Li X.P., Rahn M. and Bucher K., 2004a. Metamorphic processes in rodingites of the Zermatt-Saas Ophiolites. Intern. Geol. Rev., 46: 28-51. https://doi.org/10.2747/0020-6814.46.1.28

Li X.P., Rahn M. and Bucher K., 2004b. Serpentinites of the Zermatt-Saas ophiolite complex and their texture evolution. J. Metam. Geol., 22: 159-177. https://doi.org/10.1111/j.1525-1314.2004.00503.x

Lombardo B., Nervo R., Compagnoni R., Messiga B., Kienast J.-R., Mevel C., Fiora L., Piccardo G.B. and Lanza R., 1978. Osservazioni preliminari sulle ofioliti metamorfiche del Monviso (Alpi Occidentali). Rend. Soc. It. Miner. Petrol., 34: 235-305.

Luoni P., Rebay G., Spalla M.I. and Zanoni D., 2018. UHP Ti-chondrodite in the Zermatt-Saas serpentinite: Constraints on a new tectonic scenario. Am. Miner., 103: 1002-1005. https://doi.org/10.2138/am-2018-6460

Luoni P., Zanoni D., Rebay G. and Spalla M.I., 2019. Deformation history of Ultra High-Pressure ophiolitic serpentinites in the Zermatt-Saas Zone, Créton, Upper Valtournanche (Aosta Valley, Western Alps). Ofioliti, 44: 111-123. https://doi.org/10.4454/ofioliti.v44i2.468

Malusà M.G., Polino R. and Martin S., 2005. The Gran San Bernardo nappe in the Aosta Valley (Western Alps): a composite stack of distinct continental crust units. Bull. Soc. Géol. Fr., 176: 417-431. https://doi.org/10.2113/176.5.417

Manzotti, P., Bosse, V., Pitra, P., Robyr, M., Schiavi, F., Ballèvre, M., 2018. Exhumation rates in the Gran Paradiso Massif (Western Alps) constrained by in situ U-Th-Pb dating of accessory phases (monazite, allanite and xenotime). Contributions to Mineralogy and Petrology 173, 24. https://doi.org/10.1007/s00410-018-1452-7

Manzotti P., Pitra P., Langlade J. and Ballèvre M., 2015. Constraining P-T conditions during thrusting of a higher pressure unit over a lower pressure one (Gran Paradiso, Western Alps). J, Metam. Geol., 33: 981-1002. https://doi.org/10.1111/jmg.12156

Martin S. and Cortiana G., 2001. Influence of the whole-rock composition on crystallisation of sodic amphiboles (Piemonte nappe, Western Alps). Ofioliti, 26: 445-456.

Martin S., Tartarotti P. and Dal Piaz G.V., 1994. The Mesozoic ophiolites of the Alps: a review. OGS / Boll. Geofis. Teor. Appl., 36: 175-220.

Mevel C., Caby R. and Kienast J.-R., 1978. Amphibolite facies conditions in the oceanic crust: example of amphibolitized flasergabbro and amphibolites from the Chenaillet ophiolite massif (Hautes Alpes, France). Earth Planet. Sci. Lett., 39: 98-108. https://doi.org/10.1016/0012-821X(78)90146-2

Michard A., Avigad D., Goffé B. and Chopin C., 2004. The high-pressure metamorphic front of the south Western Alps (Ubaye–Maira transect, France, Italy). Schweiz. Miner. Petrogr. Mitt., 84: 215-235.

Michard A., Goffé B., Chopin C. and Henry C., 1996. Did the Western Alps develop through an Oman-type stage? The geotectonic setting of high-pressure metamorphism in two contrasting Tethyan transects. Ecl. Geol. Helv., 89: 43-80.

Myers J.S., 1978. Formation of banded gneisses by deformation of igneous rocks. Precamb. Res., 6: 43-64.

Nicolas A., 1966. Étude pétrochimique des roches vertes et de leurs minéraux entre Dora Maïra et Grand Paradis (Alpes piémontaises). PhD Thesis, Univ. Grenoble. Fac. Sci..

Nicollet C., Paquette J.-L., Bruand E., Bosse V. and Pereira I., 2022. Crystallisation and fast cooling of the (meta)gabbro from the Chenaillet ophiolite (Western Alps): In-situ U Pb dating of zircon, titanite, monazite and xenotime in textural context. Lithos, 414-415: 106620. https://doi.org/10.1016/j.lithos.2022.106620

Passchier C.W., Myers J.S. and Kröner A., 1990. Field geology of high-grade gneiss terrains. Springer Berlin Heidelberg.. https://doi.org/10.1007/978-3-642-76013-6

Passchier C.W. and Trouw R.A.J., 2005. Microtectonics. Springer.

Pognante U. and Sandrone R., 1989. Eclogites in the Northern Dora-Maira Nappe (Western Alps, Italy). Miner. Petroll., 40: 57-71. https://doi.org/10.1007/BF01162469

Polino R., Dal Piaz G.V. and Gosso G., 1990. Tectonic erosion at the Adria margin and accretionary processes for the Cretaceous orogeny of the Alps. Mém. Soc. Géol. Fr., 156: 345-367.

Pollard D.D. and Fletcher R.C., 2005. Fundamentals of Structural Geology, Cambridge.

Rahn M. and Bucher K., 1998. Titanian clinohumite formation in the Zermatt-Saas ophiolites, Central Alps. Miner. Petrol., 64: 1-13. https://doi.org/10.1007/BF01226561

Ramsay J.G., 1967. Folding and Fracturing of rocks. McGraw-Hill, New York.

Ramsay J.G. and Huber M.I., 1983. The techniques of modern structural geology. Acad. Press, London.

Rebay G., Spalla M.I. and Zanoni D., 2012. Interaction of deformation and metamorphism during subduction and exhumation of hydrated oceanic mantle: Insights from the Western Alps. J. Metam. Geol., 30: 687-702. https://doi.org/10.1111/j.1525-1314.2012.00990.x

Rebay G., Zanoni D., Langone A., Luoni P., Tiepolo M. and Spalla M.I., 2018. Dating of ultramafic rocks from the Western Alps ophiolites discloses Late Cretaceous subduction ages in the Zermatt-Saas Zone. Geol. Mag., 155: 298-315. https://doi.org/10.1017/S0016756817000334

Reddy S.M., Wheeler J. and Cliff R.A., 1999. The geometry and timing of orogenic extension: an example from the Western Italian Alps. J. Metam. Geol., 17: 573-589.

Reinecke T., 1991. Very high pressure metamorphism and uplift of coesite-bearing metasediments from the Zermatt-Saas Zone, Western Alps. Eu. J. Miner., 3: 7-17.

Roda M., De Salvo F., Zucali M. and Spalla M.I., 2018a. Structural and metamorphic evolution during tectonic mixing: is the Rocca Canavese Thrust Sheet (Italian Western Alps) a subduction-related mélange? It. J. Geosci., 137: 311-329. https://doi.org/10.3301/IJG.2018.17

Roda M., Regorda A., Spalla M.I. and Marotta A.M., 2018b. What drives Alpine Tethys opening? Clues from the review of geological data and model predictions. Geol. J. 54: 2646-2664 . https://doi.org/10.1002/gj.3316

Roda M., Spalla M.I. and Marotta A.M., 2012. Integration of natural data within a numerical model of ablative subduction: a possible interpretation for the Alpine dynamics of the Austroalpine crust. J. Metam. Geol., 30: 973-996. https://doi.org/10.1111/jmg.12000

Roda M. and Zucali M., 2011. Tectono-metamorphic map of the Mont Morion Permian metaintrusives (Mont Morion - Mont Collon - Matterhorn Complex, Dent Blanche Unit), Valpelline - Western Italian Alps. J. Maps, 7: 519-535. https://doi.org/10.4113/jom.2011.1194

Roda M., Zucali M., Regorda A. and Spalla M.I., 2020. Formation and evolution of a subduction-related mélange: The example of the Rocca Canavese Thrust Sheets (Western Alps). GSA Bull., 132: 884-896. https://doi.org/10.1130/B35213.1

Rolland Y., Lardeaux J.-M., Guillot S. and Nicollet C., 2000. Extension syn-convergence, poinçonnement vertical et unités métamorphiques contrastées en bordure ouest du Grand Paradis (Alpes Franco-Italiennes). Geodin. Acta, 13: 133-148. https://doi.org/10.1016/S0985-3111(00)00111-X

Rubatto D., Gebauer D. and Compagnoni R., 1999. Dating of eclogite-facies zircons: the age of Alpine metamorphism in the Sesia-Lanzo Zone (Western Alps). Earth Planet. Sci. Lett., 167: 141-158. https://doi.org/10.1016/S0012-821X(99)00031-X

Saccani E., Dilek Y., Marroni M. and Pandolfi, L., 2015. Continental margin ophiolites of Neotethys: remnants of ancient Ocean-Continent Transition Zone (OCTZ) Lithosphere and their geochemistry, mantle sources and melt evolution patterns. Episodes 38. https://doi.org/10.18814/epiiugs/2015/v38i4/82418

Salvi F., Spalla M.I., Zucali M. and Gosso G., 2010. Three-dimensional evaluation of fabric evolution and metamorphic reaction progress in polycyclic and polymetamorphic terrains: a case from the Central Italian Alps. Geol. Soc. London Spec. Publ., 332: 173-187. https://doi.org/10.1144/SP332.11

Sandrone R., Cadoppi P., Sacchi R. and and Vialon P., 1993. The Dora-Maira Massif. In: J.F. von Raumer and F. Neubauer (Eds.), Pre-Mesozoic geology in the Alps. Springer Verlag, Berlin, Heidelberg, p. 317-325.

Sandrone R., Leardi L., Rossetti P. and Compagnoni R., 1986. P-T conditions for the eclogitic re-equilibration of the metaophiolites from Val d'Ala di Lanzo (internal Piemontese zone, Western Alps). J. Metam. Geol., 4: 161-178.

Sandrone R., Sacchi R., Cordola M., Fontan D. and Villa I., 1988. Meta-diorites in the Dora Maira polymetamorphic basement (Cottian Alps). Rend. Soc. It. Miner. Petrol., 43: 593-608.

Schmid S.M., Fügenschuh B., Kissling E. and Schuster R., 2004. Tectonic map and overall architecture of the Alpine orogen. Ecl. Geol. Helv., 97: 93-117.

Schwartz S., Lardeaux J.-M., Guillot S. and Tricart, P., 2000. Diversité du métamorphisme éclogitique dans le massif ophiolitique du Monviso (Alpes occidentales, Italie). Geodin. Acta, 13: 169-188. https://doi.org/10.1080/09853111.2000.11105371

Skora S., Lapen T.J., Baumgartner L.P., Johnson C.M., Hellebrand E. and Mahlen N.J., 2009. The duration of prograde garnet crystallization in the UHP eclogites at Lago di Cignana, Italy. Earth Planet. Sci. Lett., 287: 402-411. https://doi.org/10.1016/j.epsl.2009.08.024

Spalla M.I., De Maria L., Gosso G., Miletto M. and Pognante U., 1983. Deformazione e metamorfismo della Zona Sesia - Lanzo meridionale al contatto con la falda piemontese e con il massiccio di Lanzo, Alpi occidentali. Mem Soc. Geol. It., 26: 499-514.

Spalla M.I., Goss, G., Siletto G.B., Di Paola S. and Magistroni C., 1998. Strumenti per individuare unità tettono-metamorfiche nel rilevamento geologico del basamento cristallino. Mem. Soc. Geol. It., 50 155–164.

136

Spalla M.I., Lardeaux J.M., Dal Piaz G.V., Gosso G. and Messiga B., 1996. Tectonic significance of Alpine eclogites. J. Geodyn., 21: 257-285. https://doi.org/10.1016/0264-3707(95)00033-X

Spalla M.I., Siletto G.B., di Paola S. and and Gosso G., 2000. The role of structural and metamorphic memory in the distinction of tectono-metamorphic units: the basement of the Como Lake in the Southern Alps. J. Geodyn., 30: 191-204. https://doi.org/10.1016/S0264-3707(99)00033-2

Spalla M.I. and Zucali M., 2004. Deformation vs. metamorphic re-equilibration heteroheneities in polymetamorphic rocks: a key to infer quality P-T-d-t path. Riv. It. Miner. Petrol., 73: 249-257.

Spalla, M.I., Zucali M., Di Paola S., and Gosso G., 2005. A critical assessment of the tectono-thermal memory of ocks and definition of tectono-metamorphic units: evidence from fabric and degree of metamorphic transformations. Geol. Soc. London Spec. Publ., 243: 227-247. https://doi.org/10.1144/GSL.SP.2005.243.01.16

Tartarotti P., Guerini S., Rotondo F., Festa A., Balestro G., Bebout G.E., Cannaò E., Epstein G.S. and Scambelluri M., 2019. Superposed sedimentary and tectonic block-in-matrix fabrics in a subducted Serpentinite Mélange (High-Pressure Zermatt Saas Ophiolite, Western Alps). Geosciences, 9: 358. https://doi.org/10.3390/geosciences9080358

Tribuzio R., Garzetti F., Corfu F., Tiepolo M. and Renna M.R., 2016. U-Pb zircon geochronology of the Ligurian ophiolites (Northern Apennine, Italy): Implications for continental breakup to slow seafloor spreading. Tectonophysics, 666: 220-243. https://doi.org/10.1016/j.tecto.2015.10.024

Turner, F.J. and Weiss L.E., 1963. Structural analysis of metamorphic tectonites. McGraw-Hill, New York.

Twiss R.J. and Moore C.H., 1992. Structural Geology, 2nd Ed., W.H. Freeman.

van Hinsbergen D.J.J., Torsvik T.H., Schmid S.M., Maţenco L.C., Maffione M., Vissers R.L.M., Gürer D. and Spakman W., 2020. Orogenic architecture of the Mediterranean region and kinematic reconstruction of its tectonic evolution since the Triassic. Gondw. Res., 81: 79-229. https://doi.org/10.1016/j.gr.2019.07.009

Vannay J.C. and Allemann R., 1990. La zone Piémontaise dans le Haut-Valtournanche (Val d'Aoste, ltalie). Ecl. Geol. Helv., 83: 21-39.

Weber S. and Bucher K., 2015. An eclogite-bearing continental tectonic slice in the Zermatt–Saas high-pressure ophiolites at Trockener Steg (Zermatt, Swiss Western Alps). Lithos, 232: 336-359. https://doi.org/10.1016/j.lithos.2015.07.010

Williams P.F., 1985. Multiply deformed terrains - problem of correlation. J. Struct. Geol., 7: 269-280.

Zanoni D., Rebay G., Bernardoni J. and Spalla M.I., 2012. Using multiscale structural analysis to infer high-/ultrahigh-pressure assemblages in subducted rodingites of the Zermatt-Saas Zone at Valtournanche, Italy. J. Virtual Expl., 41, 6. https://doi.org/10.3809/jvirtex.2011.00290

Zanoni D., Rebay G. and Spalla M.I., 2016. Ocean floor and subduction record in the Zermatt-Saas rodingites, Valtournanche, Western Alps. J. Metam. Geol., 34: 941-961. https://doi.org/10.1111/jmg.12215

Zucali M., Corti L., Delleani F., Zanoni D. and Spalla M.I., 2020. 3D reconstruction of fabric and metamorphic domains in a slice of continental crust involved in the Alpine subduction system: the example of Mt. Mucrone (Sesia-Lanzo Zone, Western Alps). Intern. J. Earth Sci. https://doi.org/10.1007/s00531-019-01807-6

Zucali M., Spalla M.I., Gosso G., 2002. Strain partitioning and fabric evolution as a correlation tool: the example of the Eclogitic Micaschists Complex in the Sesia-Lanzo Zone (Monte Mucrone-Monte Mars, Western Alps, Italy). Schweiz. Miner. Petrogr. Mitt., 82: 429-454.